Tokunaga, R., Takahashi, Y., Touj, S., Hotta, H., Leblond, H., Kato, F., & Piché, M. (2022). Attenuation of widespread hypersensitivity to noxious mechanical stimuli by inhibition of GABAergic neurons of the right amygdala in a rat model of chronic back pain. European Journal of Pain, 26(4), 911-928. https://doi.org/10.1002/ejp.1921

Received: 20 September 2021 | Accepted: 6 February 2022

DOI: 10.1002/ejp.1921

ORIGINAL ARTICLE

Attenuation of widespread hypersensitivity to noxious mechanical stimuli by inhibition of GABAergic neurons of the right amygdala in a rat model of chronic back pain

Ryota Tokunaga[1,2] | **Yukari Takahashi**[3] | **Sara Touj**[1,2] | **Harumi Hotta**[4] | **Hugues Leblond**[1,2] | **Fusao Kato**[3] | **Mathieu Piché**[1,2]

[1]Department of Anatomy, Université du Québec à Trois-Rivières, Trois-Rivières, Québec, Canada

[2]CogNAC Research Group, Université du Québec à Trois-Rivières, Trois-Rivières, Québec, Canada

[3]Department of Neuroscience, Jikei University School of Medicine, Tokyo, Japan

[4]Department of Autonomic Neuroscience, Tokyo Metropolitan Institute of Gerontology, Tokyo, Japan

Correspondence
Mathieu Piché, Department of Anatomy, Université du Québec à Trois-Rivières, 3351 boul. des Forges, C.P. 500, Trois-Rivières, QC, Canada G9A 5H7.
Email: mathieu.piche@uqtr.ca

Funding information
This work was supported by a grant from the Natural Sciences and Engineering Research Council of Canada (MP: grant #06659). The contribution of MP was supported by the Fonds de recherche du Québec en Santé (FRQS) and the Japan Foundation for the Promotion of Science (Grant for the Promotion of Joint International Research (Fostering Joint International Research (B)) of KAKENHI). The contribution of RT was supported by the International University of Health and Welfare and the Foundation de Recherche en Chiropratique du Québec.

Abstract

Background: Chronic primary low back pain may be associated with hyperalgesia in uninjured tissues and with decreased pain inhibition. Previous studies have shown that the amygdala is involved in pain regulation and chronic pain, that neuronal activity in the amygdala is altered in models of persistent pain, and that the central nucleus of the right amygdala plays an active role in widespread hypersensitivity to noxious stimuli.

Methods: Behavioral, electrophysiological, biochemical, and chemogenetic methods were used to examine the role of the central nucleus of the right amygdala in hypersensitivity to noxious stimuli in a rat model of chronic back pain induced by a local injection of Complete Freund Adjuvant (CFA) in paraspinal muscles.

Results: CFA produced chronic inflammation limited to the injected area. CFA-treated rats showed increased pain-like (liking) behaviors during the formalin test compared with controls. They also showed widespread mechanical hypersensitivity compared with controls, which persisted for 2 months. This widespread hypersensitivity was accompanied by altered activity of different types of right amygdala neurons, as shown by extracellular recordings. Plasmatic levels of IL-1β, IL-6, and TNF-α were not elevated after 1 or 2 months, indicating that persistent widespread hypersensitivity is not caused by persistent systemic inflammation. However, chemogenetic inhibition of GABAergic neurons in the right amygdala attenuated widespread mechanical hypersensitivity.

Conclusions: These findings indicate that chronic widespread mechanical hypersensitivity in a model of chronic back pain can be attenuated by inhibiting GABAergic neurons of the right amygdala, and that widespread hypersensitivity is not maintained by chronic systemic inflammation.

Significance: The amygdala is a key structure involved in pain perception and modulation. The present results indicate that the GABAergic neurons of its central nucleus are involved in widespread hypersensitivity to noxious stimuli in a rat model of chronic back pain. The inhibition of amygdala GABAergic neurons

may be a potential target for future interventions in patients with chronic back pain.

1 | INTRODUCTION

Chronic primary low back pain (CPLBP) may be associated with hyperalgesia in uninjured tissues (O'Neill et al., 2007, 2011) and altered pain regulation mechanisms (McPhee et al., 2020). Previous studies suggest that the amygdala is involved in diffuse noxious inhibitory controls (DNIC) and conditioned pain modulation (CPM) (Piché et al., 2009, 2014; Sprenger et al., 2011). DNIC and CPM produce widespread *hypoalgesia* (LeBars et al., 1979; Yarnitsky, 2010). Therefore, maladaptive plasticity in the amygdala may contribute to widespread pain and *hyperalgesia*.

The amygdala is involved in emotion, pain processing, pain regulation, and chronic pain (Kato et al., 2018; Neugebauer, 2015; Neugebauer et al., 2004; Palazzo et al., 2008; Phelps & LeDoux, 2005). The emotional component of pain is processed by the central nucleus of the amygdala (CeA) (Ji et al., 2007; Neugebauer et al., 2009). The capsular division of the lateral CeA (CeLC) is the main terminal of ascending nociceptive inputs originating from nociceptive-specific neurons in lamina I of the spinal cord, through the lateral parabrachial nucleus (LPB) (Basbaum et al., 2009; Bernard et al., 1989, 1993; Sarhan et al., 2005; Todd, 2010). The CeA also receives inputs from the basolateral amygdala (BLA), a nucleus that integrates polymodal sensory information from the thalamus and cortex (Neugebauer, 2015; Neugebauer et al., 2009; Thompson & Neugebauer, 2017, 2019). The medial division of the CeA (CeM) is its main output to other limbic regions and the brainstem, for behavioral responses and pain regulation, which can be influenced by the CeLC via a network of reciprocally connected GABAergic interneurons (Ciocchi et al., 2010; Duvarci & Pare, 2014; Fadok et al., 2017).

Consistent with the role of the CeA in widespread hyperalgesia in humans, its nociceptive neurons have large receptive fields, some of which respond to stimuli applied on most parts of the body (Bernard et al., 1992). In addition, synaptic transmission in the CeA is potentiated in rat models of muscle pain (Neugebauer et al., 2003; Sugimura et al., 2016) and neuropathic pain (Cheng et al., 2011; Ikeda et al., 2007). The right CeA also plays an active role in widespread hypersensitivity to noxious stimuli induced by acute inflammatory orofacial pain (Sugimoto et al., 2021). Collectively, these findings indicate that the CeA may contribute to chronic pain and widespread hyperalgesia in CPLBP.

The aim of this study was to examine the role of the CeA in widespread hypersensitivity to noxious stimuli in a rat model of chronic back pain (Touj et al., 2017). Assessment of mechanical sensitivity and extracellular recordings in the CeA were used to confirm widespread hypersensitivity and altered nociceptive processing. To rule out the contribution of systemic inflammation, plasmatic pro-inflammatory cytokines were measured after widespread hypersensitivity developed. Based on previous studies showing that the regulation of CeA GABAergic neurons modulates sensitivity to noxious stimuli (Hasanein et al., 2008; Sugimoto et al., 2021), we hypothesized that chemogenetic inhibition of CeA GABAergic neurons would attenuate chronic widespread hypersensitivity.

2 | METHODS

2.1 | Animals

All experimental procedures were approved by institutional animal care committees (Université du Québec à Trois-Rivières and Jikei University) and conformed to the ARRIVE guidelines, the Guidelines of the Canadian Council on Animal Care, the Guidelines for Proper Conduct of Animal Experiments of the Science Council of Japan, and the Guidelines of the Committee for Research and Ethical Issues of the International Association for the Study of Pain (IASP). Experiments 1 (20 animals) and 2 (24 animals) were performed on adult male Wistar rats (body weight: 330–370 g; Charles River Laboratories). Rats were kept two per cage in the animal facilities of Université du Québec à Trois-Rivières under a 14 h–10 h light–dark cycle. Food and water were available ad libitum. Experiment 3 was performed on 10 VGAT-Cre rats [W-Tg(Slc32a1-cre)3_5Fusa]. Rats were kept three per cage in the animal facilities of Jikei University, under a 12 h light–dark cycle. Food and water were available ad libitum.

2.2 | Experimental design

The experimental design is illustrated in Figure 1. In Experiment 1, mechanical sensitivity was assessed using the von Frey test over a 2-month period following an intramuscular injection of either CFA or saline into the back muscles, in order to confirm that widespread hypersensitivity to noxious stimuli was persistent and stable. At the end of this period, extracellular recordings were used to examine somatosensory responses of CeA neurons and changes in the activity of those

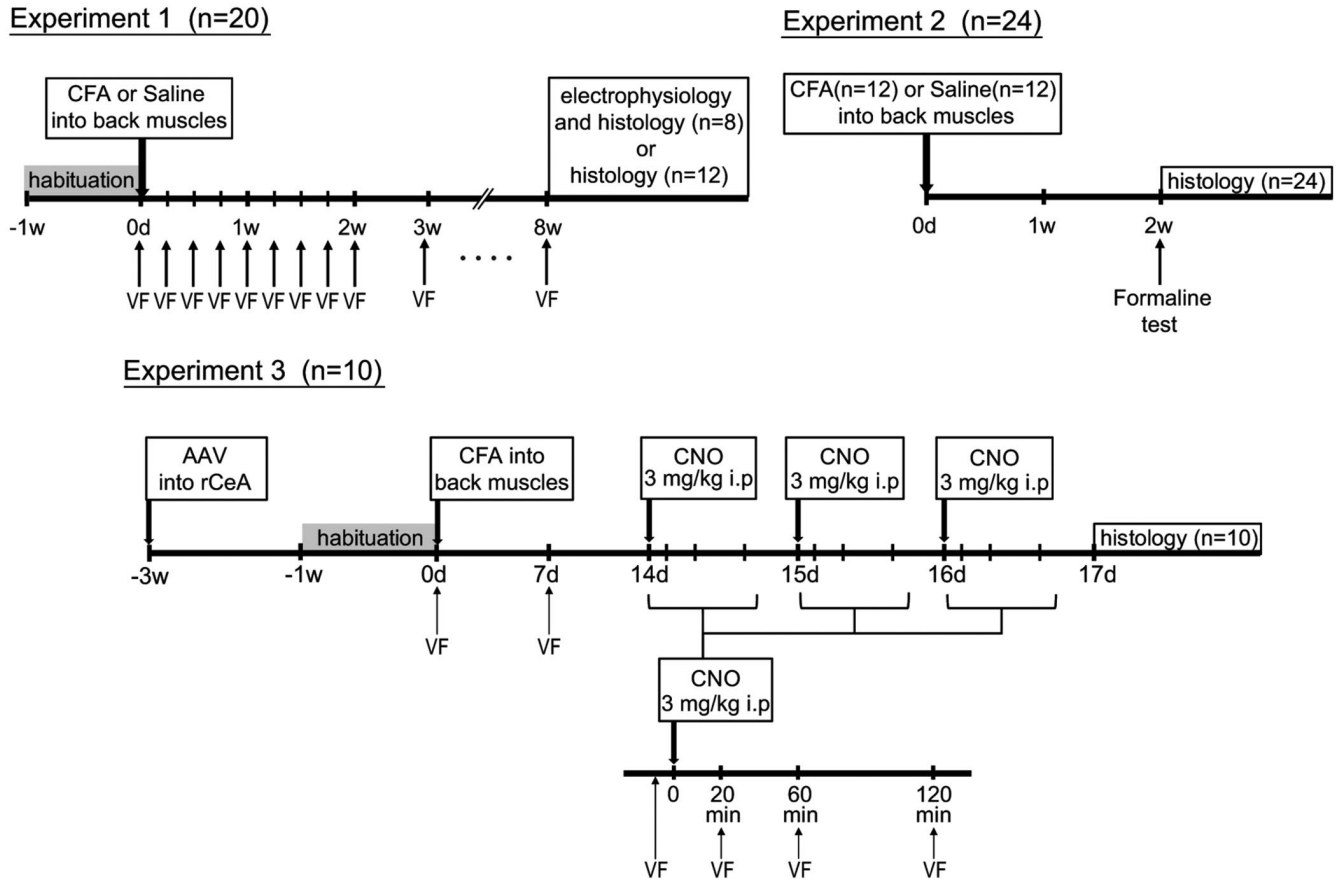

FIGURE 1 Experimental design. Experiment 1. Twenty rats were assigned to one of the two groups ($n = 10$ per group). After 1 week of daily habituation in the test cage, baseline mechanical sensitivity was assessed (von Frey test). On this day, either CFA or saline was injected into the back muscles. For the next 2 months, mechanical sensitivity was assessed once a week. After 2 months, all rats were perfused through the heart for histological assessment of muscle inflammation. In 8 of the 20 rats, electrophysiological recordings were made in the right CeA before perfusion. Experiment 2. Twenty-four rats were assigned to one of the two groups ($n = 12$ per group), for which either CFA or saline was injected into the back muscles. Two weeks later, formalin test was conducted. All rats were then perfused through the heart for histological assessment of muscle inflammation. Experiment 3. Ten rats were assigned to one of the two groups. Either AAV5_hSyn-DIO-hM4D(Gi)-mCherry or AAV5_hSyn-DIO-mCherry (control virus) was injected into the right CeA. Three weeks later, including 1 week of daily habituation in the test cage, baseline mechanical sensitivity was assessed (von Frey test). On this day, CFA was injected into the back muscles of all rats. In order to confirm the development of widespread mechanical hypersensitivity, the mechanical sensitivity was assessed on Days 0, 7, 14, 15, and 16. On Days 14, 15, and 16, the chemogenetic manipulation was also conducted. Clozapine N-oxide (CNO) was injected intraperitoneally once per day for 3 consecutive days. After CNO injection, mechanical sensitivity was assessed at 20, 60, and 120 min. VF, von Frey test

neurons due to chronic back muscle inflammation. In Experiment 2, the formalin test was performed 2 weeks after an intramuscular injection of either CFA or saline into the back muscles in order to examine whether chronic back muscle inflammation produced changes in pain-like behaviors. In Experiment 3, inhibition of CeA GABAergic neurons was performed with chemogenetic tools to assess if it could attenuate widespread hypersensitivity to noxious stimuli induced by chronic back muscle inflammation.

Based on the stable mechanical hypersensitivity from Day 7, the present experiments could all have been conducted 2 weeks after CFA injection. However, one of the objectives of the present study was to confirm that hypersensitivity persisted in the long term. This is important to validate the present model as a model of chronic back pain. Electrophysiology was conducted on these animals (Experiment 1) to examine changes in CeA neuron activity in a chronic state, but not on animals used for chemogenetics (Experiment 3). For the combination of unitary recordings and chemogenetic methods, the recording electrode should be inserted into the same local region where DREADDs are expressed and can be affected by a designer ligand. Therefore, the interpretation of unitary discharge modulation by the influence of DREADDs would be complicated and was not performed in this study.

2.3 | Chronic back pain model

Chronic back muscle inflammation was induced by intramuscular injection of Complete Freund Adjuvant (CFA; Mycobacterium tuberculosis; 0.15 mg/0.15 ml; Difco Lab.), as described previously (Touj et al., 2017). Under isoflurane anesthesia (4% inhalation for induction and 2%–2.5% for maintenance), a 27-gauge needle was inserted through the skin into the left T2 paraspinal muscles and kept in place for 3 min after injection of 150 μl of CFA. The same procedures were used for control rats, but a 150 μl solution of sterile saline (0.9%) was injected instead of CFA.

2.4 | Behavioral assessment

2.4.1 | Mechanical sensitivity (von Frey test)

In rats from Experiments 1 and 3, mechanical sensitivity was assessed for both hind paws with the von Frey test. The experimenter was blind to the experimental group, and tests were conducted by the same trained experimenter, following previously reported methods (Kim & Chung, 1992). Mechanical stimulation was performed using 11 von Frey filaments (0.4, 0.6, 1, 1.4, 2, 4, 6, 8, 10, 15, and 26 g). Testing began with the 4 g filament. Rats were placed in a homemade cage with metal mesh floor (20 × 20 cm). Before the protocol began, rats were habituated to the testing cage for 1 week by placing them in the cage daily for at least 15 min. Before each von Frey test, they were placed in the testing cage at least 15 min before the assessment. Von Frey filaments were applied manually through the mesh floor on the mid-plantar area of hind paws. Values of the paw withdrawal threshold were estimated by the up–down method (Dixon, 1980).

2.4.2 | Formalin test

In rats from Experiment 2, pain-like behaviors were assessed using the formalin test 2 weeks after the intramuscular injection of either CFA or saline into the back muscles. After a 1-h habituation period in the test cage, 50 μl of a 5% formalin solution was injected subcutaneously into the left dorsal hind paw using a 26-gauge needle. Animals were placed back into their cage immediately after the formalin injection and were observed by two trained experimenters over 45 min. The test score was determined by calculating the number of paw lickings for each 5-min interval. For quantification purposes, three phases were examined: First phase (0–10 min), Early Second phase (20–30 min), and Late Second phase (30–45 min) (Shinohara et al., 2017).

2.5 | Blood sampling and measurement of plasmatic pro-inflammatory cytokines

Under isoflurane anesthesia (4% for induction and 2%–2.5% for maintenance), blood samples were collected in animals from Experiment 1, from the left or right jugular vein (1.0–1.5 ml/sampling) into EDTA-coated vacutainer tubes using a 23-gauge needle at 1 month and 2 months after the intramuscular injection of either CFA or saline into the back muscles. The samples were kept on ice and centrifuged at 1300 g for 10 min at 4°C (Immufuge). The supernatant (plasma) was then placed in aliquots and stored at −80°C until the enzyme-linked immunosorbent assay (ELISA) was performed. The plasmatic concentration of pro-inflammatory cytokines (IL-1β, IL-6, TNF-α (soluble isoform)) was measured using commercially available ELISA kits (Quantikine, R&D). A positive control experiment was performed with one of the three cytokines. A standard solution of IL-1β was added into some of the samples, followed by the same procedures including freezing (−80°C) and all other procedures for quantification. The expected values were measured, confirming that cytokines could be detected if present in blood samples.

2.6 | Electrophysiological recordings and analyses

Surgical procedures were initiated after animals were deeply anesthetized with isoflurane (4% inhalation for induction and 2%–2.5% for maintenance). In addition to stable systemic mean arterial pressure (MAP), the depth of anesthesia was routinely confirmed during the surgery by the absence of flexion reflexes. The right femoral vein was catheterized for intravenous injections and MAP was continuously recorded from the right femoral artery with an intra-arterial cannula connected to a pressure transducer (Harvard Apparatus). Animals were artificially ventilated (SAR-830/P Ventilator, CWE Inc.) using a tracheal cannula to maintain end-tidal CO_2 between 3.0% and 3.5% (CAPSTAR-100 Carbon dioxide analyzer, CWE Inc.). Body temperature was monitored with a rectal probe (TCAT-2LV controller, Physitemp Instruments Inc.) and maintained at 37.5 ± 0.5°C with a custom-made temperature control system that prevents electrophysiological artifacts. Rats were placed in a stereotaxic frame (Model 900, Kopf Instruments) and a craniotomy was performed (antero-posteriorly from Bregma and medio-laterally from the midline at A–P: −1.5 to −3.5 mm and L: −3 to −5 mm) to allow recordings of CeA neurons. After the dura mater was removed, warm paraffin oil was applied on the brain and was re-applied during the experiment as needed.

Using a micromanipulator (Model 960, David Kopf Instruments), a 32-channel electrode (Model A1x32-Poly10 mm-50–177, NeuroNexus Technologies Inc.; impedance 0.5–1.0 MΩ; thickness of 50 μm; width of 125 μm; 32 recording sites with a center-to-center separation of 50 μm) was inserted into the right CeA for all animals (A–P: −2.4 to −2.8 mm, L: −3.9 to −4.5 mm depth: −7.2 to −8.0 from the dura). The signal was sampled at 20 kHz (SmartBox, NeuroNexus Technologies Inc.) with a broad band (band pass 1–10,000 Hz, gain: 192 V/V) and recorded for offline analyses using a personal computer. To determine the recording site, a single pulse of 1 ms at 9.6 mA was delivered to the sciatic nerve every 3 s while multi-unit activity was monitored with a loudspeaker. The electrode was moved by 100 μm steps. The recording site was selected when multi-unit activity could be clearly evoked by sciatic stimulation.

For offline analyses, the raw signal was filtered (band pass 300–10,000 Hz) to examine single-unit activity. Single-unit activity was isolated using spike sorting (Spike2 software v.6.15, Cambridge Electronic Design). Single-unit responses were plotted using peristimulus histograms (PSTH) and classified into four response types depending on spike rate increase or decrease.

For electrical stimulation, the left sciatic nerve was exposed, submerged in warm mineral oil, and mounted on a custom-made bipolar stimulation electrode connected to a constant-current stimulator (Model DS7A, Digitimer Ltd). The stimulation consisted of 1 ms pulses applied every 3 s. Intensity was changed every 50 pulses. A pause of 90 s was taken between each intensity to allow response recovery before the subsequent intensity. Eleven intensities were delivered in ascending or descending sequences (0.01, 0.05, 0.075, 0.1, 0.15, 0.3, 0.6, 1.2, 2.4, 4.8, 9.6 mA or the reverse), and sequences were counterbalanced between animals to limit intensity order effects.

2.7 | Chemogenetic experiment

A chemogenetic approach was used to inhibit CeA GABAergic neurons specifically, using designer receptors exclusively activated by designer drugs (DREADD). The methods for the chemogenetics are essentially the same as previously reported (Sugimoto et al., 2021). In brief, VGAT-cre rats were anesthetized with a subcutaneous solution (medetomidine hydrochloride (0.3 mg/kg; Zenoaq, Orion Corporation), midazolam (4.0 mg/kg; Astellas), and butorphanol tartrate (5.0 mg/kg; Meiji Seika Pharma)), and a solution of 700 nl containing an adeno-associated virus vector (AAV5-hSyn-DIO-hM4D(Gi)-mCherry or AAV5_hSyn-DIO-mCherry; (Penn Vector Core) was injected at a rate of 100 nl/min into the right CeA, using standard sterile stereotaxic procedures (AP: −2.1 mm; ML: −4.0 mm; DV: −8.0 mm from Bregma). The solution was injected using a 2-μl Hamilton syringe with a 30-gauge needle (Neuros Model 7002 KH point style 3) and a microinjection pump (UMP-4; World Precision Instruments). The solutions also contained FluoSphere (1.25%, F-8794, 0.04 mm; Molecular Probes, Thermo Fisher Scientific) for post-mortem confirmation of the injection site. After 1 week of the recovery period, rats received CFA injections into the back muscles as described above. Rats were injected clozapine-N-oxide (CNO; 3 mg/kg) intraperitoneally on Days 14, 15, and 16, and mechanical sensitivity was assessed at 20, 60, and 120 min after CNO injection (see Figure 1a). After CNO experiments, the brain was collected following transcardiac perfusion of a 10% formalin solution and post-fixed (>24 h at 4°C). Coronal 100-μm-thick sections were made with a vibrating tissue slicer (PRP7; Dosaka EM) after embedding with 1.6% agar. The fluorescence signals of mCherry and FluoSphere were visualized using a fluorescent microscope (BX-63; Olympus) and captured with a high-sensitivity CCD camera (DP-72; Olympus). The image files were stored in TIFF format and registered using bright-field images onto a reference atlas (Paxinos & Watson, 2005) using PowerPoint (369 or 2019, MicroSoft) with the highest resolution mode (i.e., no resolution downsizing). The fluorescence channel was then extracted and analyzed with IgorPro (8.0 and 9.0; WaveMetrics) to prepare half-transparent above-the-threshold images using home-made procedures, which were overlaid onto the reference atlas in PowerPoint as described previously (Sugimoto et al., 2021).

2.8 | Muscle histology

At the end of the protocol, all rats were perfused through the heart with a 10% formalin solution under isoflurane anesthesia. The left thoracic paraspinal muscles were removed and stored in a 10% formalin solution for 24 h and then preserved in phosphate buffer. Tissues were dehydrated, cleared, and embedded in paraffin (tissue processor, Tissue Tek VIP E300, Sakura Finetek). Serial sections of 5 μm in thickness were then cut using a rotary microtome (Reichert Histostat microtome model 820, Reichert Technologies) and were mounted onto adhesive-coated slides. Finally, sections were stained with a hematoxylin-phloxine-saffron coloration (Autostainer XL, Leica Microsystems) for histologic examination under a microscope.

2.9 | Statistical analyses

Statistical analyses were performed with Statistica v.13.0 (Dell Inc.). All data are expressed as mean ± SEM. Values

of $p \leq 0.05$ were considered to be statistically significant. In Experiment 1, mechanical sensitivity was compared between groups over time using a mixed ANOVA ($2 \times 2 \times 15$), with group (2) as between-subject factor, and paw (2) and time (15) as within-subject factors. For cytokines, groups were compared over time using mixed ANOVAs (2×2), with group (2) as between-subject factor and time (2) as within-subject factor. For electrophysiology, the baseline spike rate was compared between groups using an independent *t*-test, while for evoked responses, the spike rate was compared between groups over intensities using mixed ANOVAs (2×11), with group (2) as between-subject factor, and intensity (11) as within-subject factor. In experiment 2, pain-like behaviors induced by formalin were compared between groups over phases using a mixed ANOVA (2×3), with group (2) as between-subject factor, and phase (3) as within-subject factor. In experiment 3, mechanical sensitivity was compared between groups over time (Days 0, 7, 14, 15, and 16) using a mixed ANOVA (2×5), with group (2) as between-subject factor, and time (5) as within-subject factor. The effect of CNO on mechanical sensitivity was also compared between groups over time (0, 20, 60, and 120 min) using a mixed ANOVA (2×4), with group (2) as between-subject factor, and time (4) as within-subject factor. Significant effects were decomposed with the Tuckey HSD test and planned contrasts as needed. Effect sizes are reported based on partial eta-squared (η_p^2).

3 | RESULTS

3.1 | Chronic muscle inflammation in CFA rats

Muscle sections were examined to confirm the presence or absence of inflammation in all animals from the three experiments. Leukocyte infiltration, mainly macrophagic and lymphoid cells, was observed in all CFA rats (2 weeks and 2 months after CFA injection). Careful examination revealed that inflammation did not extend beyond, and was limited to, the injected area. No sign of inflammation was observed in any of the control rats. Representative examples of muscle sections from one control rat and one CFA rat are shown in Figure 2. Additional individual examples for each group are shown in Figure S1.

3.2 | Persistent widespread mechanical hypersensitivity in CFA rats

In Experiment 1, mechanical sensitivity was compared between groups over time with a mixed ANOVA (see Figure 3). Mechanical thresholds significantly decreased over time in CFA rats compared with control rats (interaction: $F_{14,252} = 4.0$, $p < 0.001$, $\eta_p^2 = 0.18$) with no significant difference between paws (interaction: $F_{14,252} = 0.7$, $p = 0.8$, $\eta_p^2 = 0.04$). The Tuckey HSD test revealed that CFA rats showed decreased pain thresholds relative to Day 0 from Day 5 until Day 56 for the left and right hind paws (all $p < 0.05$). In contrast, pain thresholds of control rats remained comparable between Day 0 and subsequent time points until Day 56, for both left and right hind paws (all $p > 0.8$).

3.3 | Widespread mechanical hypersensitivity is not caused by persistent systemic inflammation

In animals from Experiment 1, plasma levels of pro-inflammatory cytokines (IL-1β, IL-6, and TNF-α) were compared between groups over time (1 and 2 months) with mixed ANOVAs (see Figure 4). IL-1β, IL-6, and TNF-α levels were just above the detection threshold and no group difference was observed for any of the three cytokines (main effect: IL-1β: $F_{1,18} = 1.0$, $p = 0.3$, $\eta_p^2 = 0.05$; IL-6: $F_{1,18} = 0.05$, $p = 0.8$, $\eta_p^2 = 0.002$; TNF-α: $F_{1,18} = 0.6$, $p = 0.5$, $\eta_p^2 = 0.03$). Moreover, no significant change occurred between groups over time (interaction: IL-1β: $F_{1,18} = 4.0$, $p = 0.06$, $\eta_p^2 = 0.18$; IL-6: $F_{1,18} = 0.3$, $p = 0.9$, $\eta_p^2 = 0.002$; TNF-α: $F_{1,18} = 1.2$, $p = 0.3$, $\eta_p^2 = 0.06$).

3.4 | Increased pain-like behaviors induced by formalin in CFA rats

In Experiment 2, 2 weeks after the injection of CFA or saline into the back muscles, pain-like behaviors induced by the formalin test were compared between groups over time with a mixed ANOVA (see Figure 5). For the entire test duration, CFA rats showed more licking behaviors compared with control rats (main effect: $F_{1,22} = 4.3$, $p = 0.049$, $\eta_p^2 = 0.16$). This effect was not significantly different between phases (interaction: $F_{2,44} = 1.5$, $p = 0.25$, $\eta_p^2 < 0.06$). However, pain behaviors were significantly greater in CFA compared with control rats in the First phase ($p = 0.049$) and the Early Second phase ($p = 0.022$), but not in the Late Second phase ($p = 0.8$).

3.5 | Altered nociceptive processing in the right CeA of CFA rats

In rats from Experiment 1, 2 months after the injection of CFA or saline into the back muscles, single-unit recordings

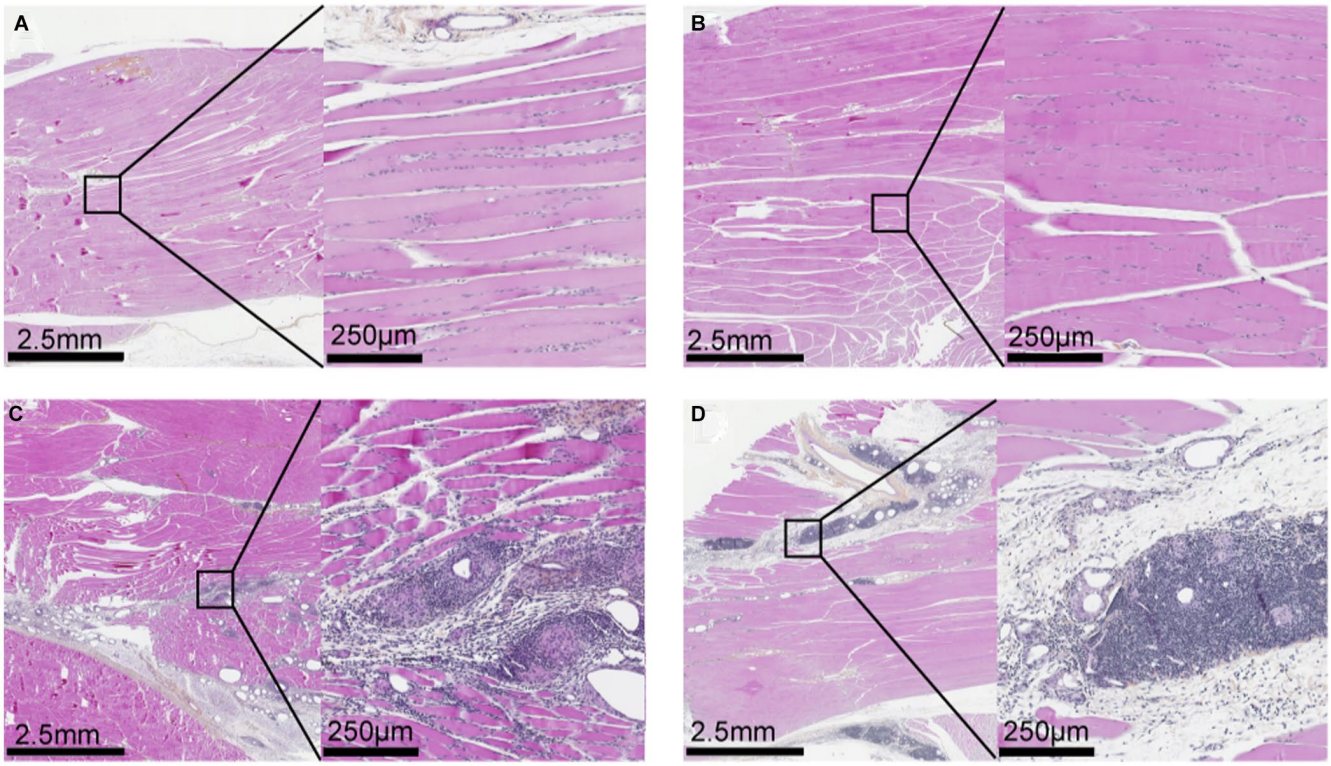

FIGURE 2 Chronic muscle inflammation induced by CFA. Representative examples of back muscle sections stained with hematoxylin, phloxine, and saffron in a control rat (a, b) and a CFA rat (c, d). Muscle sections from control rats show normal skeletal muscle fibers with no evidence of cellular damage, interstitial edema, or inflammatory reaction (a) 2 weeks or (b) 2 months after the intramuscular injection of saline. Muscle section from CFA rats 2 weeks after the intramuscular injection of CFA (c) shows interstitial edema spreading out muscle fascicles, accompanied by chronic inflammation and cystic changes characteristic of fat necrosis. At higher magnification, clusters of inflammatory cells are observed, consisting of medium-sized monocytes and darkly stained lymphocytes. Fat necrosis foci appear as cystic spaces surrounded by a typical histiocytic and giant cell inflammatory reaction. Of note, lymphocytic cells are percolating through individual eosinophilic muscle fibers. Muscle section from CFA rats 2 months after the intramuscular injection of CFA (d) shows prominent interstitial edema interspersed with cystic spaces and clusters of chronic inflammatory cells. At higher magnification, evident inflammation consists mainly of darkly stained lymphocytes but also contains medium-sized monocytes surrounding empty-looking clear spaces typical of fat necrosis. When compared with (c), interstitial edema is more pronounced while lymphocytic infiltrate between individual fibers is hardly seen

were performed in 8 rats (4 controls and 4 CFA). A total of 300 responsive neurons were isolated in control rats and 502 in CFA rats. The classification of neurons by response type is presented in Table 1. In controls, 256 neurons (85.3%) showed an increased spike rate and 44 neurons (14.7%) showed a decreased spike rate in response to electrical stimulation of the sciatic nerve. In CFA rats, 467 neurons (93.0%) showed an increased spike rate and 35 neurons (7.0%) showed a decreased spike rate in response to sciatic stimulation. Individual examples of the four types of neurons are shown in Figure 6a–d. An increased spike rate was observed as a short monophasic spike rate increase (within 20 ms post-stimulus) (Type I; CFA: 41.8%; CTL: 35.0% of the total number of neurons), a biphasic spike rate increase with an early peak within 20 ms, and a late peak between 100 and 200 ms post-stimulus (Type II; CFA: 41.2%; CTL: 32.0% of the total number of neurons), or a sustained spike rate increase between 0 and 300 ms post-stimulus (Type III; CFA: 10.0%; CTL: 18.3% of the total number of neurons). The decreased spike rate was always observed as a sustained spike rate decrease between 100 and 1000 ms post-stimulus (Type IV; CFA: 7.0%; CTL: 14.7% of the total number of neurons).

In order to compare the response characteristics of these neurons between groups, baseline activity and intensity-response curves were compared between CFA and control rats for each of the four types of neurons (see Table 2 and Figure 6e–i).

For Type I neurons, the baseline spike rate was comparable between CFA and control rats ($p = 0.92$). As for the response to sciatic stimulation, the spike rate increased with intensity (main effect: $F_{10,\ 3130} = 231.3$, $p < 0.001$, $\eta_p^2 = 0.42$) and this effect was significantly different between groups, where CFA rats showed an increased spike rate compared with control rats (interaction: $F_{10,\ 3130} = 11.1$, $p < 0.001$, $\eta_p^2 = 0.03$). Bonferroni-planned

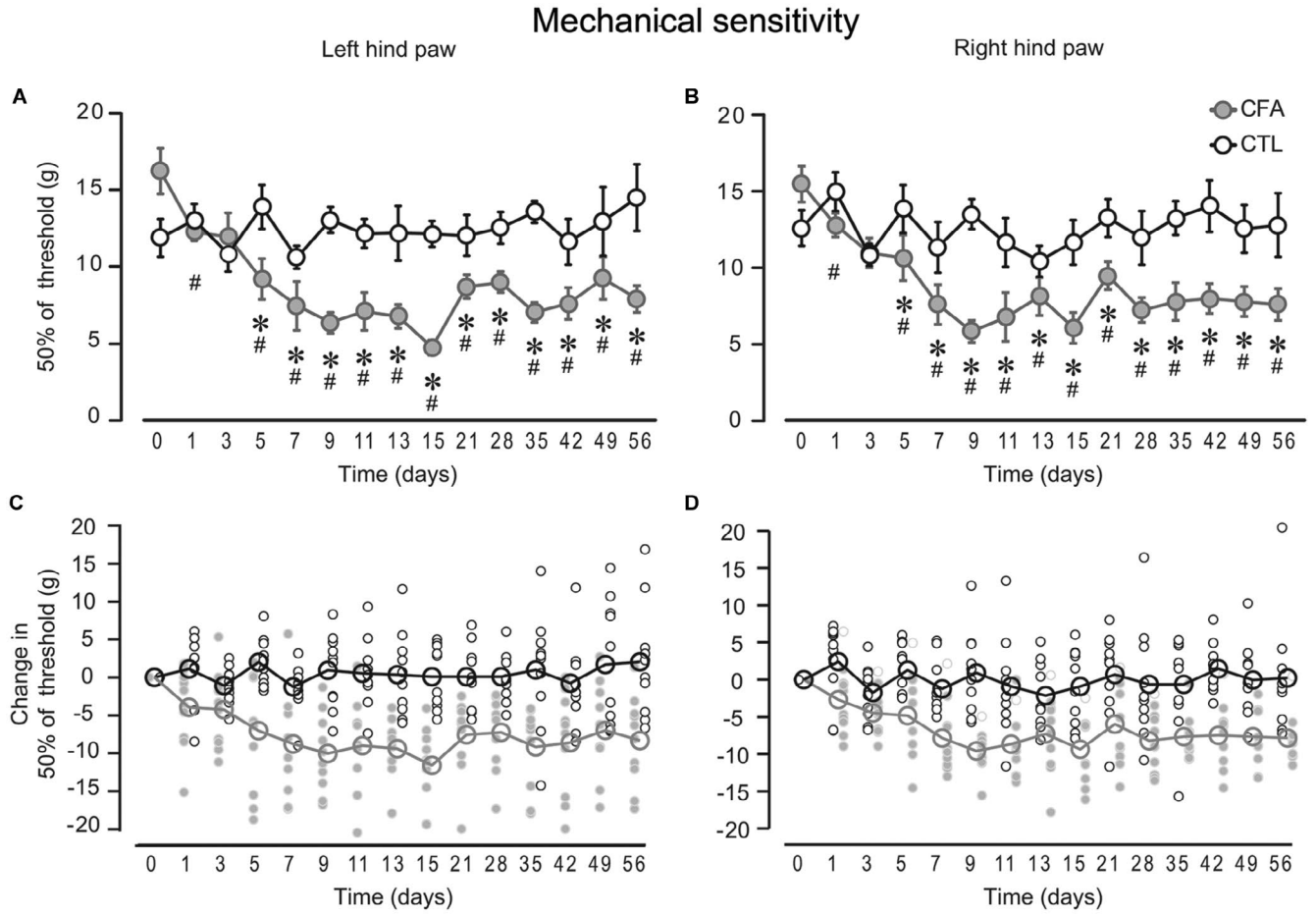

FIGURE 3 Mechanical sensitivity (von Frey test). Time course of mechanical sensitivity over 2 months, following either CFA ($n = 10$) or saline ($n = 10$) injection into the back muscles. (a, b) show raw values, while (c, d) show standardized values relative to baseline (change in sensitivity), with individual data points for all rats from both groups. Mechanical sensitivity significantly decreased over time in CFA rats compared with control rats (interaction: $p < 0.001$) with no significant difference between paws ($p = 0.8$; see a, b). The Tuckey HSD test revealed that CFA rats showed increased mechanical sensitivity (decreased threshold), relative to Day 0, from Day 5 until Day 56 for the left and right hind paws (all $p < 0.05$; see gray circles in (a, b), as indicated by the * symbol). In contrast, mechanical sensitivity in control rats remained comparable between Day 0 and subsequent time points until Day 56 for both left and right hind paws (all $p > 0.8$; see white circles in (a, b), respectively). In addition, mechanical thresholds in the CFA group were significantly lower compared with those in the control group for both the left and right hind paws, for Day 1, and from Day 5 until Day 56 (all $p < 0.05$; see (a, b), as indicated by the # symbol). In panels (c, d), individual data are shown as changes relative to baseline over time for illustration purposes. Negative values indicate mechanical hypersensitivity. In (a, b), error bars indicate the standard error of the mean. *$p < 0.05$ within group compared with baseline (simple effect); $^{\#}p < 0.05$ between groups for each time point compared with baseline (interaction)

contrasts revealed that CFA rats showed a greater spike rate compared with control rats for intensities between 0.05 and 0.15 mA (all $p < 0.001$) but not for higher intensities (all $p > 0.1$).

For Type II neurons, the baseline spike rate was comparable for neurons from CFA and control rats ($p = 0.43$). As for the response to electrical stimulation, both components of the biphasic response were analyzed. The spike rate was lower in CFA rats compared with control rats for the first peak (main effect: $F_{1,\,301} = 9.2$, $p < 0.01$, $\eta_p^2 = 0.03$) and the second peak (main effect: $F_{1,\,301} = 14.4$, $p < 0.01$, $\eta_p^2 = 0.05$). Moreover, the spike rate increased with intensity for both components (first component: main effect: $F_{10,\,3010} = 162.4$, $p < 0.001$, $\eta_p^2 = 0.35$; second component: main effect: $F_{10,\,3010} = 136.1$, $p < 0.001$, $\eta_p^2 = 0.01$), and these effects were significantly different between groups (first component: interaction: $F_{10,\,3010} = 3.7$, $p < 0.001$, $\eta_p^2 = 0.01$; second component: interaction: $F_{10,\,3010} = 8.1$, $p < 0.001$, $\eta_p^2 = 0.03$). For the first component, Bonferroni-planned contrasts revealed that neurons from CFA rats showed a lower spike rate compared with those from control rats for intensities between 0.075 and 0.15 mA (all $p < 0.05$), but not for the other intensities (all $p > 0.1$). For the second component, Bonferroni-planned contrasts revealed that neurons from CFA rats showed a lower spike rate compared

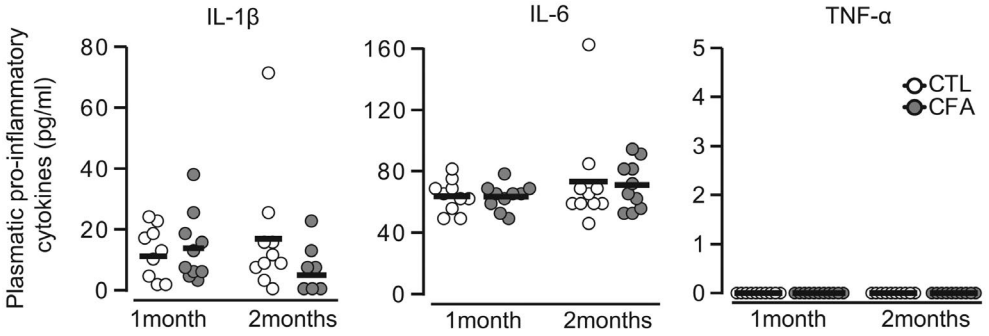

FIGURE 4 Systemic inflammation. Plasma levels of pro-inflammatory cytokines (IL-1β, IL-6, and TNF-α) at 1 and 2 months for control rats ($n = 10$) and CFA rats ($n = 10$). IL-1β, IL-6, just above the detection threshold and TNF-α was at the detection threshold with very low concentrations. No group difference was observed for any of the three cytokines (all $p > 0.3$). Moreover, no significant change occurred between groups over time (all $p > 0.05$). Individual data are represented by white and gray filled circles, and the mean is represented by a horizontal black bar

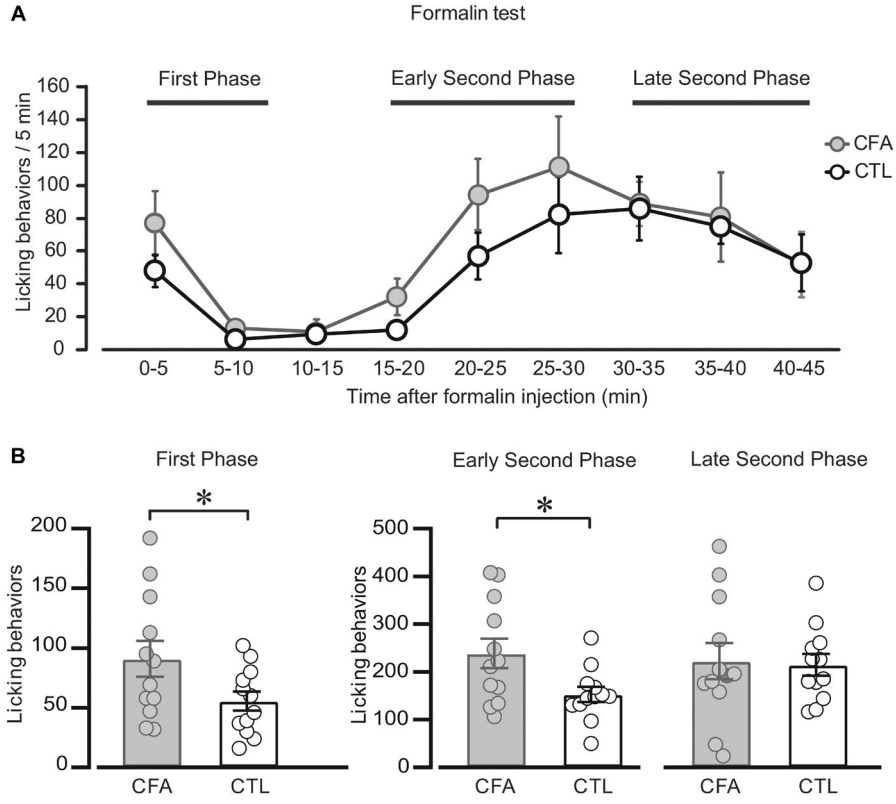

FIGURE 5 Pain-like behaviors during the formalin test. (a) Time course of pain-like (licking) behaviors after subcutaneous injection of formalin into the left dorsal hind paw in CFA ($n = 12$) and control ($n = 12$) rats. (b) Cumulative licking behaviors in the First (0–10 min), Early Second (15–30 min), and Late Second (30–45 min) phases following formalin injection. CFA rats showed more licking behaviors compared with control rats in the First phase ($p = 0.049$) and the Early Second phase ($p = 0.022$), but not in the Late Second phase ($p = 0.8$). Gray and white circles represent individual data. Error bars indicate the standard error of the mean. *$p < 0.05$

with those from control rats for 0.075, 0.1, 0.15, and 9.6 mA (all $p < 0.05$), but not for the other intensities (all $p > 0.1$).

For Type III neurons, the baseline spike rate was lower in neurons from CFA rats compared with those from control rats ($p = 0.002$). As for the response to electrical stimulation, the spike rate was lower in CFA rats compared with control rats (main effect: $F_{1, 103} = 9.0$, $p < 0.01$, $\eta_p^2 = 0.08$). Moreover, the spike rate increased with intensity (main effect: $F_{10, 1030} = 86.6$, $p < .001$, $\eta_p^2 = 0.46$) and this effect was significantly different between groups (interaction: $F_{10, 1030} = 6.6$, $p < 0.001$, $\eta_p^2 = 0.06$). Bonferroni-planned contrasts revealed that neurons from CFA rats showed a lower spike rate compared with those from control rats for 2.4, 4.8, and 9.6 mA intensities (all $p < 0.05$) but not for the other intensities (all $p > 0.1$).

TABLE 1 Classification of neurons based on response type

	CFA (*n*)	CTL (*n*)	CFA (%)	CTL (%)
Type I	210	105	41.8	35.0
Type II	207	96	41.2	32.0
Type III	50	55	10.0	18.3
Type IV	35	44	7.0	14.7
Total	502	300	100	100

For Type IV neurons, the baseline spike rate was greater in neurons from CFA rats compared with those from control rats ($p < 0.001$). As for the response to electrical stimulation, the spike rate decrease was greater in CFA rats compared with control rats (main effect: $F_{1, 77} = 18.1$, $p < 0.001$, $\eta_p^2 = 0.19$). Moreover, the spike rate differed between intensities (main effect: $F_{10, 770}$=38.8, $p < 0.001$, $\eta_p^2 = 0.33$) and this effect was significantly different between groups (interaction: $F_{10, 770} = 17.1$, $p < 0.001$, $\eta_p^2 = 0.18$). Bonferroni-planned contrasts revealed that neurons from CFA rats showed a greater spike rate decrease compared with those from control rats for 0.15, 2.4, 4.8, and 9.6 mA intensities (all $p < 0.05$) but not for the other intensities (all $p > 0.1$).

3.6 | Attenuation of widespread mechanical hypersensitivity by chemogenetic inhibition of CeA GABAergic neurons

Chemogenetic inhibition of CeA GABAergic neurons was performed in VGAT-Cre rats (see Figure 1 for experimental protocol). VGAT-Cre rats were distributed into hM4D-mCherry ($n = 5$) and mCherry (control) ($n = 5$) groups. All rats from both groups received a CFA injection into the back muscles as described above. Mechanical sensitivity was compared between groups over time (Days 0, 7, 14, 15, and 16) using a mixed ANOVA. Mechanical thresholds decreased over time (main effect: $F_{4,32} = 8.8$, $p < 0.001$, $\eta_p^2 = 0.52$) with no significant difference between groups (interaction: $F_{4,32} = 1.8$, $p = 0.16$, $\eta_p^2 = 0.18$) and no significant difference between paws (interaction: $F_{4,32} = 3.0$, $p = 0.08$, $\eta_p^2 = 0.28$). The Tuckey HSD test revealed that mechanical thresholds were significantly decreased on Days 7, 14, 15, and 16 for both hind paws combined and for each hind paw separately (all $p < 0.01$; see Figure 7). This indicates that both groups showed persistent widespread mechanical hypersensitivity and that baseline pain thresholds were not modified by repeated CNO administration on 3 days (Day 14–16).

Regarding the acute effect of CNO, mechanical thresholds were compared between groups over time (0, 20, 60, and 120 min) using a mixed ANOVA. Mechanical thresholds were significantly different between groups over time following CNO injection (interaction: $F_{3,24} = 3.2$, $p = 0.04$, $\eta_p^2 = 0.29$) with no significant difference between paws (interaction: $F_{3,24} = 0.5$, $p = 0.7$, $\eta_p^2 = 0.06$) (see Figure 8). The Tuckey post hoc test revealed that for both hind paws combined, the hM4D-mCherry group showed a significantly reduced mechanical hypersensitivity after 60 min ($p < 0.001$) but not after 20 min ($p = 0.11$) or 120 min ($p = 0.18$), compared with time 0. For each hind paw separately, the hM4D-mCherry group showed a significantly reduced mechanical hypersensitivity after 20 ($p = 0.028$), 60 ($p < 0.001$), and 120 ($p = 0.05$) minutes compared with time 0 for the left hind paw, and after 60 min ($p < 0.001$) but not 20 ($p = 0.27$) or 120 ($p = 0.48$) minutes compared with time 0 for the right hind paw. By contrast, the mCherry group showed no change at any time point relative to time 0 for both hind paws combined or the left and right hind paws separately (all $p = 1.0$).

To confirm the infection of CeA GABAergic neurons by the AAV, m-Cherry expression was examined in the brain of each animal. In each rat, m-Cherry expression was observed in the CeA, sometimes extending into the BLA and sometimes extending into other surrounding regions (see Figure 9).

4 | DISCUSSION

In the present study, CFA rats showed widespread hypersensitivity that persisted over 2 months. Secondary hypersensitivity to noxious stimuli has also been reported in several animal models in which unilateral injury to a hind limb leads to hypersensitivity to noxious stimuli in both the ipsilateral and contralateral limbs (Bileviciute et al., 1993; Coderre & Melzack, 1985; Fitzgerald, 1982). Moreover, inflammation in one gastrocnemius muscle produces mechanical hypersensitivity in both paws (Sabharwal et al., 2016). In these models, secondary hypersensitivity can be caused by spinal or cerebral processes. In the present study, rats with chronic back muscle inflammation showed mechanical hypersensitivity at both hind limbs, from which sensory afferents project to the lumbosacral spinal cord. However, chronic inflammation was in the back, from which sensory afferents project to the upper thoracic spinal cord. This excludes segmental processes and indicates that widespread hypersensitivity was likely caused by cerebral processes.

In addition to mechanical hypersensitivity, CFA rats showed increased pain-like (licking) behaviors during the formalin test. We observed licking behaviors following intraplantar formalin injection in both groups, but CFA rats showed more licking behaviors than controls. This complement findings from the von Frey test and together the behavioral results indicate that evoked and spontaneous pain-like behaviors are increased in CFA rats.

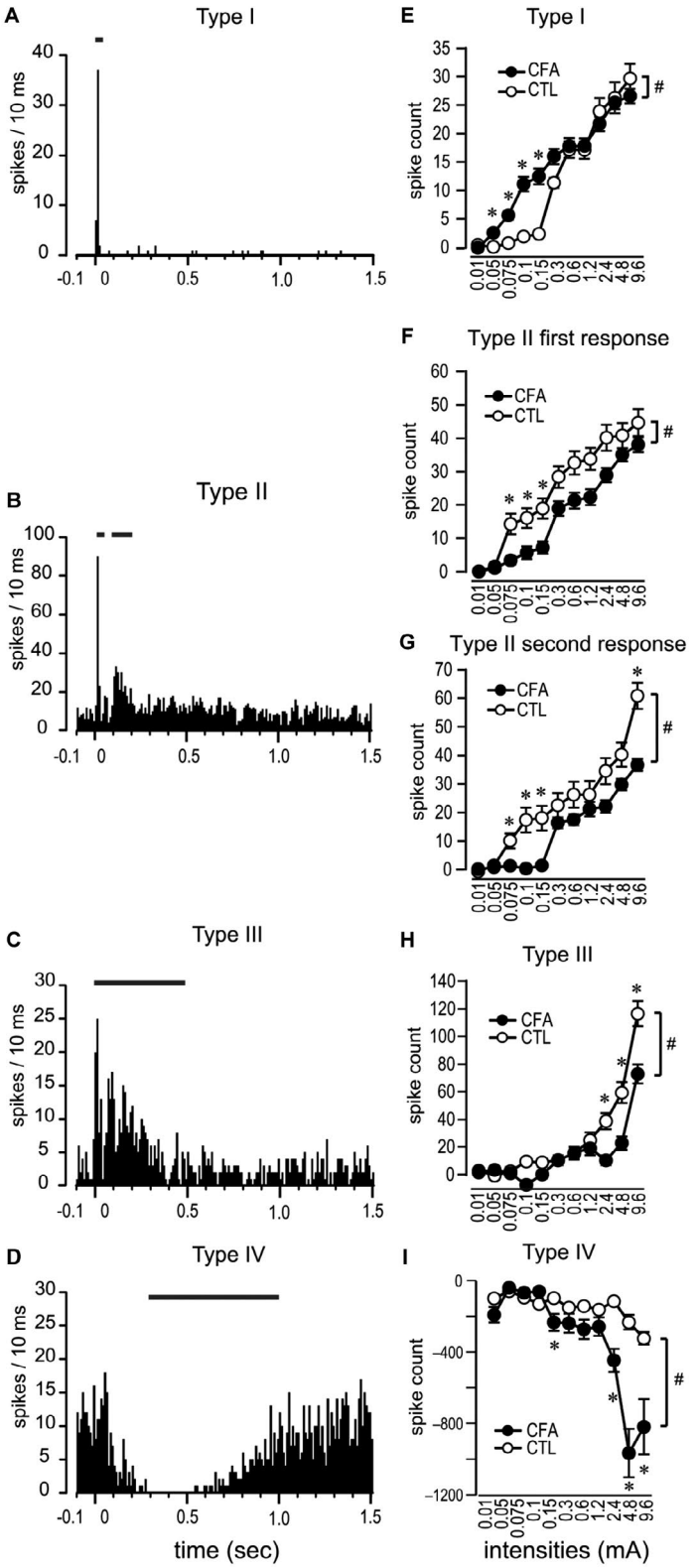

FIGURE 6 Neuronal responses in the right CeA to stimulation of left sciatic nerve. Neurons were classified according to four types of responses (a–d). (a) Individual example of a Type I neuron showing the peri-stimulus time histogram (PSTH; bin with 10 ms) at a stimulation intensity of 9.6 mA. A short monophasic spiking increase was observed within 20 ms post-stimulus. (b) Individual example of a Type II neuron showing the PSTH at a stimulation intensity of 9.6 mA. A biphasic spiking increase was observed as an early response within 20 ms and a late response between 100 and 200 ms post-stimulus. (c) Individual example of a Type III neuron showing the PSTH at a stimulation intensity of 9.6 mA. A sustained spiking increase was observed between 0 and 300 ms post-stimulus. (d) Individual example of a Type IV neuron showing the PSTH at a stimulation intensity of 9.6 mA. A sustained spiking decrease was observed between 100 and 1000 ms post-stimulus. (e–i). Intensity-response curves were built for each neuron and averaged for each of the four response types. Horizontal bars in (a–d) indicate the time window for the calculation of the intensity-response curves. For all response types, the intensity-response curves were significantly different between groups ($p < 0.001$), showing either stronger (e, i) or weaker responses (f–h) in CFA compared with control rats. $^{*}p < 0.05$ between groups. $^{\#}p < 0.001$ for the main effect of group. Error bars indicate the standard error of the mean

TABLE 2 Baseline activity (mean spike count/10 ms over 1000 ms; mean ± SEM)

Classification	CFA	CTL	*p*-value	Effect size η_p^2	Change
Type I	1.36 ± 0.08	1.38 ± 0.12	0.92	<0.01	—
Type II	1.54 ± 0.10	1.40 ± 0.15	0.43	<0.01	—
Type III	1.02 ± 0.23	1.97 ± 0.19	0.002	0.09	Decreased in CFA
Typy IV	2.85 ± 0.28	1.24 ± 0.25	<0.001	0.2	Increased in CFA

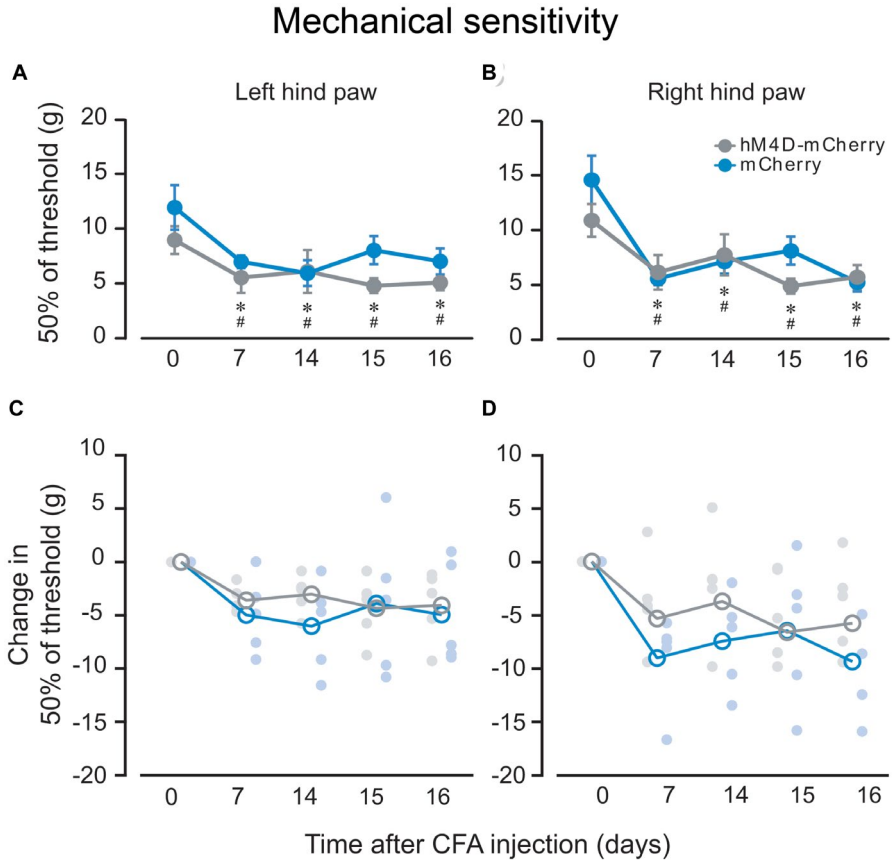

FIGURE 7 Widespread mechanical hypersensitivity in the chemogenetic experiment. (a, b) Animals from both groups (hM4D-mCherry and mCherry) showed widespread mechanical hypersensitivity after intramuscular CFA injection on Days 7, 14, 15, and 16 for both hind paws combined or for each hind paw separately (all $p < 0.01$), in spite of repetitive CNO administration on Days 14, 15, and 16. (c, d) The change in mechanical threshold showed in (a, b) is represented with gray and blue lines (means) and gray and blue circles (individual data) for illustration purposes. * and # $p < 0.01$ for hM4D-mCherry and mCherry groups, respectively. Error bars indicate the standard error of the mean

4.1 | Is widespread hypersensitivity caused by systemic inflammation?

Injection of musculoskeletal tissues with CFA is a common approach to study musculoskeletal pain mechanisms (Ambalavanar et al., 2006; Asgar et al., 2015). When injected in muscles or fascia, a low dose of CFA induces chronic inflammation in a limited area of the injected tissues (Decaris et al., 1999; Touj et al., 2017). In the present study, a low dose of CFA was used to induce chronic back muscle inflammation and local chronic inflammatory changes persisted for at least 2 months. Although chronic inflammation was induced locally, widespread hypersensitivity developed and persisted over 2 months. Thus, the possibility that systemic inflammation may maintain widespread mechanical hypersensitivity should be considered. It is well known that pro-inflammatory cytokines such as tumor necrosis factor (TNF)-α, IL-1β, and IL-6 contribute to the development of inflammatory and neuropathic pain (Sorkin et al., 1997; Zhang & An, 2007; Zhang et al., 2002). In the present study, plasmatic IL-1β, IL-6, and TNF-α were not increased in CFA rats compared with controls, 1 or 2 months after CFA injection. This confirms that widespread hypersensitivity was not maintained by persistent systemic inflammation. This does not exclude that systemic inflammation was present earlier (Decaris et al., 1999), but indicates that changes in the central nervous system are more likely to explain the

FIGURE 8 Attenuation of widespread hypersensitivity by chemogenetic manipulation of the CeA. Mechanical sensitivity was significantly different between groups over time following CNO injection ($p = 0.04$), with no significant difference between paws ($p = 0.7$). The Tuckey post hoc test revealed that for both hind paws combined, the hM4D-mCherry group showed reduced mechanical sensitivity (increased threshold) after 60 min ($p < 0.001$) but not after 20 min ($p = 0.11$) or 120 min ($p = 0.18$), compared with time 0. For each hind paw separately, the hM4D-mCherry group showed reduced mechanical sensitivity after 20 ($p = 0.028$), 60 ($p < 0.001$), and 120 ($p = 0.05$) minutes compared with time 0 for the left hind paw (a), and after 60 min ($p < 0.001$) but not 20 ($p = 0.27$) or 120 ($p = 0.48$) minutes compared with time 0 for the right hind paw (b). By contrast, the mCherry group showed no change in mechanical sensitivity at any time point relative to time 0 for both hind paws combined or the left and right hind paws separately (a, b; all $p = 1.0$). In (a, b), the thick gray and blue lines represent the mean of each group for the 3 days, which are represented separately by pale pink and blue lines. For (c–h), all individual data and means are presented for each day, each time point, each group, and each hind paw for illustration purposes. *$p < 0.05$ ***$p < 0.001$. Error bars indicate the standard error of the mean

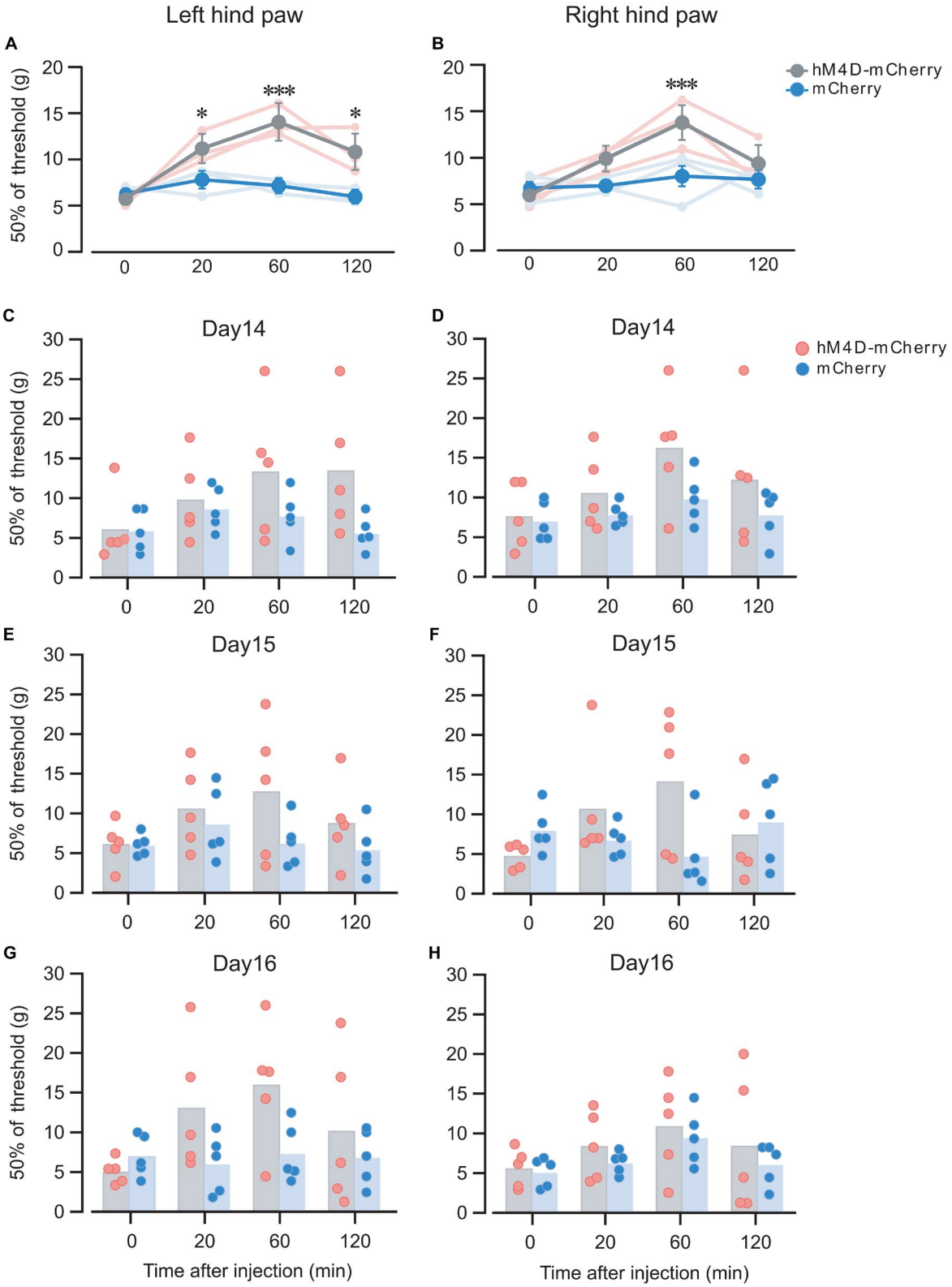

persistent widespread hypersensitivity. Another possibility to examine in a future study is the sustained microglial activation in the area postrema, as shown in mice with collagen-induced arthritis (Matsushita et al., 2021), which may produce the release of cytokines in the brain and contribute to the present findings.

4.2 | Altered neuronal activity in the right amygdala

Electrophysiological recordings in the right CeA showed four types of neuronal responses to sciatic stimulation (see Section 3). According to the latencies, Type I

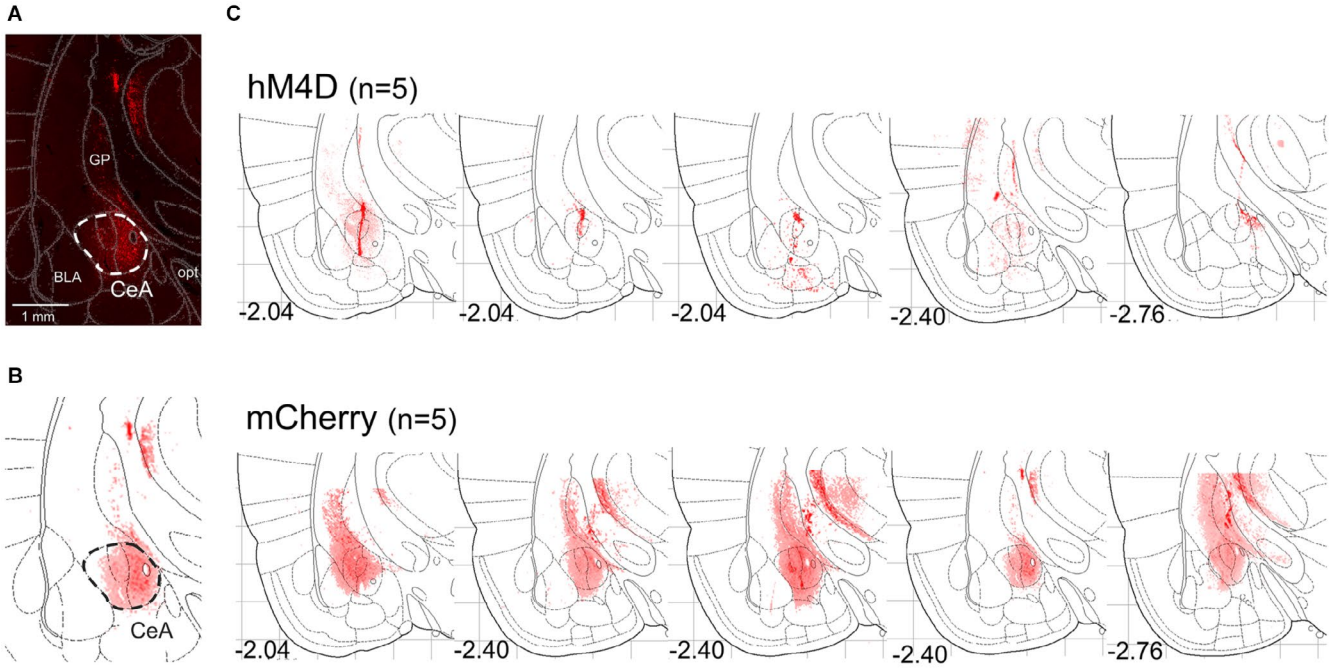

FIGURE 9 Histological verification of the area with DREADD expression. (a) A representative epifluorescence micrograph of a slice containing the central amygdala and surrounding structures. Red signal indicates the fluorescence of mCherry, which was expressed together with hM4D or alone, following AAV injection into the right amygdala. (b) The fluorescence signal was overlaid onto a representative atlas (Paxinos & Watson, 2005) after carefully registering the brain tissue image to the atlas. The area with a low level or no fluorescence was detected by thresholding and masking. (c) Detected fluorescence signal from the five hM4D-mCherry rats (upper panels) and the five mCherry only (lower panels). The numbers at the bottom of panels indicate the anterior–posterior coordinates from Bregma. Note that the fluorescence signal levels were lower with the AAV vector for hM4D than that for mCherry only, which is in agreement with our previous report using the same transgenic rat strain and the same AAV vector (Sugimoto et al., 2021). This may be the result of the longer hM4D+mCherry sequences compared with mCherry alone, and it was shown that this lower fluorescence level does not affect the ligand-evoked responses critically (Sugimoto et al., 2021)

responses and the early component of Type II responses are consistent with the activation of A-delta fibers projecting to CeA via LPB (Bernard et al., 1992), or directly from the spinal cord (Cliffer et al., 1991; Menetrey & De Pommery, 1991). The late component of Type II responses is consistent with the activation of C fibers projecting to CeA via LPB, or the activation of A-delta fibers projecting to CeA via multisynaptic pathways. These responses are similar to those reported earlier by Bernard et al. (1992), who also reported neurons with responses that outlasted stimulus application and neurons that showed a long-lasting inhibition (Type III and IV neurons in the present study).

A novel finding of the present study is that these responses were altered in CFA rats. The increased spike rate responses were either enhanced (Type I) or decreased (Types II and III), and the decreased spike rate responses were increased, especially at high intensity. Moreover, spontaneous activity was decreased for Type III neurons and increased for type IV neurons. This indicates that the excitability and responses of the CeA neurons are altered by chronic back muscle inflammation. The heterogeneity of responses suggests that these neurons have different functions, in accordance with previous studies (Amano et al., 2012; Wilson et al., 2019). For example, nerve injury sensitizes CeA neurons that express protein kinase C delta (CeA-PKCd), which increases pain-related responses, while CeA neurons that express somatostatin (CeA-Som) are inhibited and produce antinociceptive effects (Wilson et al., 2019). Accordingly, chemogenetic activation of CeA-PKCd neurons and chemogenetic inhibition of CeA-SOM neurons induce mechanical hypersensitivity at both hind paws in naive mice (Wilson et al., 2019), while the excitability of CeA-SOM neurons is decreased in a neuropathic pain model (Wilson et al., 2019). However, it should be considered that the CeA is involved in emotions and the emotional component of pain (Phelps & LeDoux, 2005; Thompson & Neugebauer, 2019), so changes in neuronal activity may also reflect anxiety and depression (Chen et al., 2021; Zhou et al., 2019). This warrants future studies to clarify which changes in neuronal activity reflect the effects of chronic pain, anxiety, and depression.

4.3 | Inhibition of right CeA GABAergic neurons attenuates persistent mechanical hypersensitivity

Chemogenetic inhibition of right CeA GABAergic neurons attenuated widespread mechanical hypersensitivity in CFA rats. This is consistent with the attenuation of widespread mechanical hypersensitivity by the inhibition of right but not left CeA GABAergic neurons in rats with acute facial inflammatory pain (Sugimoto et al., 2021). The predominant role of the right amygdala in inflammatory pain has been reported previously. For example, increased c-Fos immunoreactivity is predominant in the right CeA in rats with bilateral inflammatory pain and bilateral activation in the LPB (Miyazawa et al., 2018). In addition, the blockade of ERK activation in the right CeA, but not the left, decreases inflammation-induced hypersensitivity independently of the side of peripheral injury (Carrasquillo & Gereau, 2008). Furthermore, increased baseline and evoked neuronal activity by experimental induction of arthritis is observed only in the right CeA (Ji & Neugebauer, 2009), while increased evoked activity is observed in the right CeA 14 days after spinal nerve ligation surgery (Goncalves & Dickenson, 2012). These findings indicate that the right CeA is predominantly activated by persistent and chronic pain and generally has a pro-nociceptive role. The present results warrant future studies to determine the pathways that are involved in producing the attenuation of mechanical hypersensitivity, whether inhibition of GABAergic neurons desensitizes other amygdala neurons, or whether they actively produce descending inhibition through projections to the periaqueductal gray (da Costa Gomez & Behbehani, 1995; LeDoux et al., 1988; Rizvi et al., 1991).

4.4 | Limitations and future directions

CNO may have nonspecific effects and it could be argued that this could explain the present results. However, this is unlikely. Indeed, in the present experimental conditions, CNO had no notable nonspecific effects and its effects through activation of hM4D receptors were significantly greater compared with the nonspecific effects, if any.

Besides, we examined the effects of CNO in CFA rats expressing hM4Di-mCherry only, for following two reasons. Firstly, the von Frey test is not sensitive enough to detect the attenuation of nocifensive responses caused by strong mechanical stimuli, in animals without hypersensitivity, in which the mechanical threshold is elevated by CNO (ceiling effect). Secondly, it is already known that activation of hM3Dq-mCherry-expressing GABAergic neurons in the CeA of VGAT-cre rats, as used in this study, is sufficient to induce mechanical hypersensitivity at the hind paw, even in the absence of inflammation (Sugimoto et al., 2021).

In the present study, the repetition of CNO injections was limited to three times on separate days. In future studies, it would be relevant to examine whether repeated CNO injections over several weeks can produce a sustained attenuation of widespread mechanical hypersensitivity and increased spontaneous pain-like behaviors.

5 | CONCLUSION

In summary, the present results show that chronic back muscle inflammation induces widespread hypersensitivity to noxious stimuli and altered neuronal activity in the CeA. Moreover, mechanical hypersensitivity was attenuated by inhibition of CeA GABAergic neurons. Considering the role of the amygdala in patients with chronic pain, the present results may be relevant to human studies.

ACKNOWLEDGMENTS

The authors would like to thank the staff of the local animal facilities for their technical help and animal care.

CONFLICTS OF INTEREST

The authors declare no competing interests and no relationship that may lead to any conflict of interest.

AUTHOR CONTRIBUTIONS

Ryota Tokunaga contributed to all aspects of the research. Sara Touj contributed to data collection and interpretation. Yukari Takahashi contributed to data collection, analyses, and interpretation. Dr. Harumi Hotta contributed to experimental design and revised the manuscript. Fusao Kato contributed to experimental design, data interpretation, and revised the manuscript. Hugues Leblond contributed to data collection and revised the manuscript. Mathieu Piché contributed to all aspects of the research, obtained funding for the study, and wrote the final version of the manuscript. All authors have approved the final version of the manuscript.

ORCID

Mathieu Piché https://orcid.org/0000-0003-4171-2226

REFERENCES

Amano, T., Amir, A., Goswami, S., & Pare, D. (2012). Morphology, PKCdelta expression, and synaptic responsiveness of different types of rat central lateral amygdala neurons. *Journal of Neurophysiology*, *108*, 3196–3205.

Ambalavanar, R., Dessem, D., Moutanni, A., Yallampalli, C., Yallampalli, U., Gangula, P., & Bai, G. (2006). Muscle inflammation induces a rapid increase in calcitonin gene-related

peptide (CGRP) mRNA that temporally relates to CGRP immunoreactivity and nociceptive behavior. *Neuroscience*, *143*, 875–884. https://doi.org/10.1016/j.neuroscience.2006.08.015

Asgar, J., Zhang, Y., Saloman, J. L., Wang, S., Chung, M. K., & Ro, J. Y. (2015). The role of TRPA1 in muscle pain and mechanical hypersensitivity under inflammatory conditions in rats. *Neuroscience*, *310*, 206–215. https://doi.org/10.1016/j.neuroscience.2015.09.042

Basbaum, A. I., Bautista, D. M., Scherrer, G., & Julius, D. (2009). Cellular and molecular mechanisms of pain. *Cell*, *139*, 267–284. https://doi.org/10.1016/j.cell.2009.09.028

Bernard, J. F., Alden, M., & Besson, J. M. (1993). The organization of the efferent projections from the pontine parabrachial area to the amygdaloid complex: A Phaseolus vulgaris leucoagglutinin (PHA-L) study in the rat. *The Journal of Comparative Neurology*, *329*, 201–229. https://doi.org/10.1002/cne.903290205

Bernard, J. F., Huang, G. F., & Besson, J. M. (1992). Nucleus centralis of the amygdala and the globus pallidus ventralis: Electrophysiological evidence for an involvement in pain processes. *Journal of Neurophysiology*, *68*, 551–569. https://doi.org/10.1152/jn.1992.68.2.551

Bernard, J. F., Peschanski, M., & Besson, J. M. (1989). A possible spino (trigemino)-ponto-amygdaloid pathway for pain. *Neuroscience Letters*, *100*, 83–88. https://doi.org/10.1016/0304-3940(89)90664-2

Bileviciute, I., Lundeberg, T., Ekblom, A., & Theodorsson, E. (1993). Bilateral changes of substance P-, neurokinin A-, calcitonin gene-related peptide- and neuropeptide Y-like immunoreactivity in rat knee joint synovial fluid during acute monoarthritis. *Neuroscience Letters*, *153*, 37–40. https://doi.org/10.1016/0304-3940(93)90071-R

Carrasquillo, Y., & Gereau, R. W.. (2008). Hemispheric lateralization of a molecular signal for pain modulation in the amygdala. *Molecular Pain*, *4*, 24. https://doi.org/10.1186/1744-8069-4-24

Chen, W. H., Lien, C. C., & Chen, C. C. (2021). Neuronal basis for pain-like and anxiety-like behaviors in the central nucleus of the amygdala. *Pain*. https://doi.org/10.1097/j.pain.0000000000002389

Cheng, S. J., Chen, C. C., Yang, H. W., Chang, Y. T., Bai, S. W., Chen, C. C., Yen, C. T., & Min, M. Y. (2011). Role of extracellular signal-regulated kinase in synaptic transmission and plasticity of a nociceptive input on capsular central amygdaloid neurons in normal and acid-induced muscle pain mice. *Journal of Neuroscience*, *31*, 2258–2270. https://doi.org/10.1523/JNEUROSCI.5564-10.2011

Ciocchi, S., Herry, C., Grenier, F., Wolff, S. B., Letzkus, J. J., Vlachos, I., Ehrlich, I., Sprengel, R., Deisseroth, K., Stadler, M. B., Muller, C., & Luthi, A. (2010). Encoding of conditioned fear in central amygdala inhibitory circuits. *Nature*, *468*, 277–282. https://doi.org/10.1038/nature09559

Cliffer, K. D., Burstein, R., & Giesler, G. J., Jr. (1991). Distributions of spinothalamic, spinohypothalamic, and spinotelencephalic fibers revealed by anterograde transport of PHA-L in rats. *Journal of Neuroscience*, *11*, 852–868. https://doi.org/10.1523/JNEUROSCI.11-03-00852.1991

Coderre, T. J., & Melzack, R. (1985). Increased pain sensitivity following heat injury involves a central mechanism. *Behavioral Brain Research*, *15*, 259–262. https://doi.org/10.1016/0166-4328(85)90181-0

da Costa Gomez, T. M., & Behbehani, M. M. (1995). An electrophysiological characterization of the projection from the central nucleus of the amygdala to the periaqueductal gray of the rat: The role of opioid receptors. *Brain Research*, *689*, 21–31. https://doi.org/10.1016/0006-8993(95)00525-U

Decaris, E., Guingamp, C., Chat, M., Philippe, L., Grillasca, J. P., Abid, A., Minn, A., Gillet, P., Netter, P., & Terlain, B. (1999). Evidence for neurogenic transmission inducing degenerative cartilage damage distant from local inflammation. *Arthritis and Rheumatism*, *42*, 1951–1960. https://doi.org/10.1002/1529-0131(199909)42:9<1951:AID-ANR22>3.0.CO;2-D

Dixon, W. J. (1980). Efficient analysis of experimental observations. *Annual Review of Pharmacology and Toxicology*, *20*, 441–462. https://doi.org/10.1146/annurev.pa.20.040180.002301

Duvarci, S., & Pare, D. (2014). Amygdala microcircuits controlling learned fear. *Neuron*, *82*, 966–980. https://doi.org/10.1016/j.neuron.2014.04.042

Fadok, J. P., Krabbe, S., Markovic, M., Courtin, J., Xu, C., Massi, L., Botta, P., Bylund, K., Muller, C., Kovacevic, A., Tovote, P., & Luthi, A. (2017). A competitive inhibitory circuit for selection of active and passive fear responses. *Nature*, *542*, 96–100. https://doi.org/10.1038/nature21047

Fitzgerald, M. (1982). Alterations in the ipsi- and contralateral afferent inputs of dorsal horn cells produced by capsaicin treatment of one sciatic nerve in the rat. *Brain Research*, *248*, 97–107. https://doi.org/10.1016/0006-8993(82)91151-9

Goncalves, L., & Dickenson, A. H. (2012). Asymmetric time-dependent activation of right central amygdala neurones in rats with peripheral neuropathy and pregabalin modulation. *European Journal of Neuroscience*, *36*, 3204–3213. https://doi.org/10.1111/j.1460-9568.2012.08235.x

Hasanein, P., Mirazi, N., & Javanmardi, K. (2008). GABAA receptors in the central nucleus of amygdala (CeA) affect on pain modulation. *Brain Research*, *1241*, 36–41. https://doi.org/10.1016/j.brainres.2008.09.041

Ikeda, R., Takahashi, Y., Inoue, K., & Kato, F. (2007). NMDA receptor-independent synaptic plasticity in the central amygdala in the rat model of neuropathic pain. *Pain*, *127*, 161–172. https://doi.org/10.1016/j.pain.2006.09.003

Ji, G., Fu, Y., Ruppert, K. A., & Neugebauer, V. (2007). Pain-related anxiety-like behavior requires CRF1 receptors in the amygdala. *Molecular Pain*, *3*, 13. https://doi.org/10.1186/1744-8069-3-13

Ji, G., & Neugebauer, V. (2009). Hemispheric lateralization of pain processing by amygdala neurons. *Journal of Neurophysiology*, *102*, 2253–2264. https://doi.org/10.1152/jn.00166.2009

Kato, F., Sugimura, Y. K., & Takahashi, Y. (2018). Pain-associated neural plasticity in the parabrachial to central amygdala circuit: Pain changes the brain, and the brain changes the pain. *Advances in Experimental Medicine and Biology*, *1099*, 157–166.

Kim, S. H., & Chung, J. M. (1992). An experimental model for peripheral neuropathy produced by segmental spinal nerve ligation in the rat. *Pain*, *50*, 355–363. https://doi.org/10.1016/0304-3959(92)90041-9

LeBars, D., Dickenson, A. H., & Besson, J. M. (1979). Diffuse noxious inhibitory controls (DNIC). I. Effects on dorsal horn convergent neurones in the rat. *Pain*, *6*, 283–304. https://doi.org/10.1016/0304-3959(79)90049-6

LeDoux, J. E., Iwata, J., Cicchetti, P., & Reis, D. J. (1988). Different projections of the central amygdaloid nucleus mediate autonomic

and behavioral correlates of conditioned fear. *Journal of Neuroscience*, *8*, 2517–2529. https://doi.org/10.1523/JNEUROSCI.08-07-02517.1988

Matsushita, T., Otani, K., Oto, Y., Takahashi, Y., Kurosaka, D., & Kato, F. (2021). Sustained microglial activation in the area postrema of collagen-induced arthritis mice. *Arthritis Research & Therapy*, *23*, 273. https://doi.org/10.1186/s13075-021-02657-x

McPhee, M. E., Vaegter, H. B., & Graven-Nielsen, T. (2020). Alterations in pronociceptive and antinociceptive mechanisms in patients with low back pain: A systematic review with meta-analysis. *Pain*, *161*, 464–475. https://doi.org/10.1097/j.pain.0000000000001737

Menetrey, D., & De Pommery, J. (1991). Origins of spinal ascending pathways that reach central areas involved in visceroception and visceronociception in the rat. *European Journal of Neuroscience*, *3*, 249–259. https://doi.org/10.1111/j.1460-9568.1991.tb00087.x

Miyazawa, Y., Takahashi, Y., Watabe, A. M., & Kato, F. (2018). Predominant synaptic potentiation and activation in the right central amygdala are independent of bilateral parabrachial activation in the hemilateral trigeminal inflammatory pain model of rats. *Molecular Pain*, *14*, 1744806918807102. https://doi.org/10.1177/1744806918807102

Neugebauer, V. (2015). Amygdala pain mechanisms. *Handbook of Experimental Pharmacology*, *227*, 261–284.

Neugebauer, V., Galhardo, V., Maione, S., & Mackey, S. C. (2009). Forebrain pain mechanisms. *Brain Research Reviews*, *60*, 226–242. https://doi.org/10.1016/j.brainresrev.2008.12.014

Neugebauer, V., Li, W., Bird, G. C., Bhave, G., & Gereau, R. W.. (2003). Synaptic plasticity in the amygdala in a model of arthritic pain: Differential roles of metabotropic glutamate receptors 1 and 5. *Journal of Neuroscience*, *23*, 52–63. https://doi.org/10.1523/JNEUROSCI.23-01-00052.2003

Neugebauer, V., Li, W., Bird, G. C., & Han, J. S. (2004). The amygdala and persistent pain. *Neuroscientist*, *10*, 221–234. https://doi.org/10.1177/1073858403261077

O'Neill, S., Kjaer, P., Graven-Nielsen, T., Manniche, C., & Arendt-Nielsen, L. (2011). Low pressure pain thresholds are associated with, but does not predispose for, low back pain. *European Spine Journal*, *20*, 2120–2125. https://doi.org/10.1007/s00586-011-1796-4

O'Neill, S., Manniche, C., Graven-Nielsen, T., & Arendt-Nielsen, L. (2007). Generalized deep-tissue hyperalgesia in patients with chronic low-back pain. *European Journal of Pain*, *11*, 415–420. https://doi.org/10.1016/j.ejpain.2006.05.009

Palazzo, E., Fu, Y., Ji, G., Maione, S., & Neugebauer, V. (2008). Group III mGluR7 and mGluR8 in the amygdala differentially modulate nocifensive and affective pain behaviors. *Neuropharmacology*, *55*, 537–545. https://doi.org/10.1016/j.neuropharm.2008.05.007

Paxinos, G., & Watson, C. (2005). *The rat brain in stereotaxic coordinates*, 5th ed. Elsevier Academic Press.

Phelps, E. A., & LeDoux, J. E. (2005). Contributions of the amygdala to emotion processing: From animal models to human behavior. *Neuron*, *48*, 175–187. https://doi.org/10.1016/j.neuron.2005.09.025

Piché, M., Arsenault, M., & Rainville, P. (2009). Cerebral and cerebrospinal processes underlying counterirritation analgesia. *Journal of Neuroscience*, *29*, 14236–14246. https://doi.org/10.1523/JNEUROSCI.2341-09.2009

Piché, M., Watanabe, N., Sakata, M., Oda, K., Toyohara, J., Ishii, K., Ishiwata, K., & Hotta, H. (2014). Basal mu-opioid receptor availability in the amygdala predicts the inhibition of pain-related brain activity during heterotopic noxious counter-stimulation. *Neuroscience Research*, *81–82*, 78–84.

Rizvi, T. A., Ennis, M., Behbehani, M. M., & Shipley, M. T. (1991). Connections between the central nucleus of the amygdala and the midbrain periaqueductal gray: Topography and reciprocity. *The Journal of Comparative Neurology*, *303*, 121–131. https://doi.org/10.1002/cne.903030111

Sabharwal, R., Rasmussen, L., Sluka, K. A., & Chapleau, M. W. (2016). Exercise prevents development of autonomic dysregulation and hyperalgesia in a mouse model of chronic muscle pain. *Pain*, *157*, 387–398. https://doi.org/10.1097/j.pain.0000000000000330

Sarhan, M., Freund-Mercier, M. J., & Veinante, P. (2005). Branching patterns of parabrachial neurons projecting to the central extended amgydala: Single axonal reconstructions. *The Journal of Comparative Neurology*, *491*, 418–442. https://doi.org/10.1002/cne.20697

Shinohara, K., Watabe, A. M., Nagase, M., Okutsu, Y., Takahashi, Y., Kurihara, H., & Kato, F. (2017). Essential role of endogenous calcitonin gene-related peptide in pain-associated plasticity in the central amygdala. *European Journal of Neuroscience*, *46*, 2149–2160. https://doi.org/10.1111/ejn.13662

Sorkin, L. S., Xiao, W. H., Wagner, R., & Myers, R. R. (1997). Tumour necrosis factor-alpha induces ectopic activity in nociceptive primary afferent fibres. *Neuroscience*, *81*, 255–262.

Sprenger, C., Bingel, U., & Buchel, C. (2011). Treating pain with pain: Supraspinal mechanisms of endogenous analgesia elicited by heterotopic noxious conditioning stimulation. *Pain*, *152*, 428–439. https://doi.org/10.1016/j.pain.2010.11.018

Sugimoto, M., Takahashi, Y., Sugimura, Y. K., Tokunaga, R., Yajima, M., & Kato, F. (2021). Active role of the central amygdala in widespread mechanical sensitization in rats with facial inflammatory pain. *Pain*, *162*, 2273–2286. https://doi.org/10.1097/j.pain.0000000000002224

Sugimura, Y. K., Takahashi, Y., Watabe, A. M., & Kato, F. (2016). Synaptic and network consequences of monosynaptic nociceptive inputs of parabrachial nucleus origin in the central amygdala. *Journal of Neurophysiology*, *115*, 2721–2739. https://doi.org/10.1152/jn.00946.2015

Thompson, J. M., & Neugebauer, V. (2017). Amygdala plasticity and pain. *Pain Research and Management*, *2017*, 1–12. https://doi.org/10.1155/2017/8296501

Thompson, J. M., & Neugebauer, V. (2019). Cortico-limbic pain mechanisms. *Neuroscience Letters*, *702*, 15–23. https://doi.org/10.1016/j.neulet.2018.11.037

Todd, A. J. (2010). Neuronal circuitry for pain processing in the dorsal horn. *Nature Reviews Neuroscience*, *11*, 823–836. https://doi.org/10.1038/nrn2947

Touj, S., Houle, S., Ramla, D., Jeffrey-Gauthier, R., Hotta, H., Bronchti, G., Martinoli, M. G., & Piche, M. (2017). Sympathetic regulation and anterior cingulate cortex volume are altered in a rat model of chronic back pain. *Neuroscience*, *352*, 9–18. https://doi.org/10.1016/j.neuroscience.2017.03.047

Wilson, T. D., Valdivia, S., Khan, A., Ahn, H. S., Adke, A. P., Martinez Gonzalez, S., Sugimura, Y. K., & Carrasquillo, Y. (2019). Dual and opposing functions of the central amygdala in the modulation of pain. *Cell Reports*, *29*(2), 332–346.e5. https://doi.org/10.1016/j.celrep.2019.09.011

Yarnitsky, D. (2010). Conditioned pain modulation (the diffuse noxious inhibitory control-like effect): Its relevance for acute and chronic pain states. *Current Opinion in Anaesthesiology*, *23*, 611–615. https://doi.org/10.1097/ACO.0b013e32833c348b

Zhang, J. M., & An, J. (2007). Cytokines, inflammation, and pain. *International Anesthesiology Clinics*, *45*, 27–37. https://doi.org/10.1097/AIA.0b013e318034194e

Zhang, J. M., Li, H., Liu, B., & Brull, S. J. (2002). Acute topical application of tumor necrosis factor alpha evokes protein kinase A-dependent responses in rat sensory neurons. *Journal of Neurophysiology*, *88*, 1387–1392.

Zhou, W., Jin, Y., Meng, Q., Zhu, X., Bai, T., Tian, Y., Mao, Y., Wang, L., Xie, W., Zhong, H., Zhang, N., Luo, M. H., Tao, W., Wang, H., Li, J., Li, J., Qiu, B. S., Zhou, J. N., Li, X., … Zhang, Z. (2019). A neural circuit for comorbid depressive symptoms in chronic pain. *Nature Neuroscience*, *22*, 1649–1658. https://doi.org/10.1038/s41593-019-0468-2

SUPPORTING INFORMATION

Additional supporting information may be found in the online version of the article at the publisher's website.

How to cite this article: Tokunaga, R., Takahashi, Y., Touj, S., Hotta, H., Leblond, H., Kato, F., & Piché, M. (2022). Attenuation of widespread hypersensitivity to noxious mechanical stimuli by inhibition of GABAergic neurons of the right amygdala in a rat model of chronic back pain. *European Journal of Pain*, 26, 911–928. https://doi.org/10.1002/ejp.1921